Hopf bifurcations in balance equations of glow discharges

B.-P. Koch, N. Goepp, and B. Bruhn
Institut für Physik, Ernst-Moritz-Arndt-Universität Greifswald, Domstrasse 10a, 17487 Greifswald, Germany
(Received 1 April 1997)

Starting from the hydrodynamic equations describing the positive column of glow discharges in inert gases, the instability of the axially homogeneous state is investigated. Dirichlet boundary conditions at the ends of the positive column are chosen. Stimulated by experiments, the influence of metastable atoms and of the outer circuit is taken into consideration by additional equations. Center manifold and normal form theories are used to characterize the codimension-one bifurcations. Depending on the current, the length of the positive column and the resistance of the outer circuit supercritical and subcritical Hopf bifurcations are found. The importance of the results with respect to the experiments on the ionization instability in a neon discharge is discussed. [S1063-651X(97)05208-2]

PACS number(s): 52.35.Py, 52.80.Hc, 05.45.+b

I. INTRODUCTION

The understanding of complex spatiotemporal behavior in extended dissipative systems far from equilibrium is one of the most challenging problems in physics. Many instabilities connected with a rich bifurcation structure are observed when the system is driven far from equilibrium [1,2]. In some fluid systems, e.g., Rayleigh-Bénard convection or Taylor-Couette flow, patterns can arise when an external stress exceeds a critical value. Also the homogeneous state of the positive column in a glow discharge in certain pressure-current ranges is unstable and the plasma changes into a spatially inhomogeneous state, i.e., the positive column is formed of bright and dark layers alternating in the longitudinal direction [3]. These so-called striations, which may be standing or moving, are generated because the destabilizing mechanisms, i.e., direct and stepwise ionization by collisions of electrons with neutral atoms and collisions between excited neutral atoms, surpass the stabilizing recombination processes. In low-pressure discharges stepwise ionization is the dominant instability mechanism. In inert gases moving striations (ionization waves) are produced with a phase velocity that is directed from the anode to the cathode, whereas the group velocity points at the anode. Beginning in the past century there are many experimental results that are dedicated to the dispersion properties and the instability regions in parameter space of ionization waves in discharges of inert and molecular gases. The most relevant contributions are reviewed by Nedospasov [4], Pekarek [5], Oleson and Cooper [6], and Landa *et al.* [7]. In the case of neon discharges Achterberg and Michel [8] and Pfau *et al.* [9] have explored the regions of existence of different types of ionization waves.

The modern experiments study the nonlinear properties of ionization waves and ionization turbulence including such phenomena as period doubling, torus deformation, chaotic behavior, and pattern formation [10–15]. A review of such papers was published by Ohe [16]. Numerical simulations of nonlinear behavior were accomplished by Grabec and Mikac [17,18] using a very truncated hydrodynamic model. The theoretical investigations in the past mostly concentrated on the linear behavior [19–25]. Almost all of these calculations were based on hydrodynamic equations. From the viewpoint of kinetic theory the fluid approach describes the electron distribution function using three parameters: density, drift velocity, and mean energy. This is justified in the high-pressure regime, where the electron-electron interaction is the dominant process and the isotropic part of the distribution function is nearly Maxwellian. In the low-pressure region, where nonlocal effects are present, a correct investigation has to start with the Boltzmann equation. Initial attempts to calculate the linear properties of ionization waves by a kinetic description of electrons were made by Rohlena, Ružička, and Pekarek [21,22] and Tsendin [23,24]. Nevertheless, because the required calculations are too involved, until now there has been no successful explanation of the nonlinear properties of ionization waves by means of the kinetic theory. Therefore, our studies are based on a fluid approximation, which is useful not only in the high-pressure regime [7]. Most of our data are taken to characterize a low-pressure neon discharge. Our aim is to describe qualitatively some of the linear and nonlinear phenomena observed in experiments.

Comparing our paper with the previous ones, the following most important extensions are realized. First, nonlinear properties of the traveling waves are calculated. Furthermore, the influence of metastable atoms and of the outer circuit is taken into account. The importance of these extensions is strongly indicated by experiments [26,27]. The bifurcations, which are realized if the system goes from a stable homogeneous state to a traveling wave state, are discussed. Codimension-one and codimension-two bifurcations are found in parameter space, but only the former are analyzed. Center manifold theory connected with normal form transformation is the mathematical method used. The basic equations are introduced in Sec. II. The terms omitted to simplify the calculations are also established. In Sec. III the linear stability problem is solved by numerical methods. Eigenvalues and eigenfunctions and their parameter dependence are calculated. Furthermore, the adjoint problem is also handled. In Sec. IV the parameter dependence of the cubic normal form coefficient that characterizes the type of bifurcation, amplitude, and nonlinear frequency shift of the wave near the stability boundary is analyzed. The results are

discussed in Sec. V. The Appendix contains data for the collision rates, transport coefficients, and additional constants.

II. BASIC EQUATIONS

We apply a hydrodynamic description of the positive column. Balance equations for the density of electrons, ions, and metastable atoms n_e, n_i, n_m are used [4]:

$$\frac{\partial n_e}{\partial t} + \mathrm{div}(n_e \vec{v_e}) = P_e, \tag{2.1}$$

$$\frac{\partial n_i}{\partial t} + \mathrm{div}(n_i \vec{v_i}) = P_i, \tag{2.2}$$

$$\frac{\partial n_m}{\partial t} + \mathrm{div}(n_m \vec{v_m}) = P_m. \tag{2.3}$$

The velocities $\vec{v_e}, \vec{v_i}, \vec{v_m}$ are obtained from the momentum balance without the inertia terms,

$$\vec{v_e} = -b_e \vec{E} - D_e \frac{\mathrm{grad}(n_e)}{n_e} - K_e \frac{\mathrm{grad}(U_{em})}{U_{em}}, \tag{2.4}$$

$$\vec{v_i} = b_i \vec{E}, \tag{2.5}$$

$$\vec{v_m} = -D_m \frac{\mathrm{grad}(n_m)}{n_m}. \tag{2.6}$$

They contain electron motion caused by the electric field $\vec{E}$, diffusion, and thermodiffusion as well as ion drift and diffusion of metastable atoms with the corresponding transport coefficients b_e, D_e, K_e, b_i, D_m. Moreover, the balance of the mean electron energy U_{em}

$$\frac{\partial (n_e U_{em})}{\partial t} + \mathrm{div}(n_e U_{em} \vec{w}) = -n_e \vec{v_e} \cdot \vec{E} - n_e H \tag{2.7}$$

includes on the right-hand side the energy changes by the electric field and the losses by elastic and inelastic collisions that are contained in H. The velocity of heat current $\vec{w}$ is given by

$$\vec{w} = -b_e^* \vec{E} - D_e^* \frac{\mathrm{grad}(n_e)}{n_e} - K_e^* \frac{\mathrm{grad}(U_{em})}{U_{em}}, \tag{2.8}$$

with the transport coefficients b_e^*, D_e^*, K_e^*. In the balance equations of density the source terms P_e, P_i, and P_m describe the gain and loss of particles by collisions and can be written as

$$P_e = z_{0\infty} n_g n_e + z_{m\infty} n_m n_e + z_A n_m^2, \tag{2.9}$$

$$P_i = z_{0\infty} n_g n_e + z_{m\infty} n_m n_e + z_A n_m^2, \tag{2.10}$$

$$P_m = z_{0m} n_g n_e - z_{mg} n_g n_m - z_{me} n_e n_m - 2 z_A n_m^2. \tag{2.11}$$

The collision rates contain the influence of direct and stepwise ionization ($z_{0\infty}, z_{m\infty}$), the ionization through collisions between metastable atoms (z_A), the production of metastable atoms through collisions of electrons with gas atoms (z_{0m}), and the loss of metastable atoms through collisions with gas atoms (z_{mg}) and electrons (z_{me}), respectively. The influence of excited gas atoms on the dynamics of charge carriers is considered by only one density n_m, which is balanced in Eq. (2.3). This is only a crude approximation with respect to the fact that the lowest group of excited levels consists of two metastable levels ($1s_3, 1s_5$) and two resonance levels ($1s_2, 1s_4$). In our basic equations we have summarized the influence of the two metastable levels. The resonance atoms are neglected. In the next step of the approximation the resonance levels should also be balanced in a proper equation. The source term in the energy balance

$$H = n_g (p_{el} + p_{0a} + p_{0\infty} + p_w) + n_m p_{a\infty} \tag{2.12}$$

includes losses by elastic (p_{el}) and inelastic collisions. The inelastic ones take excitation (p_{0a}), direct ionization ($p_{0\infty}$), stepwise ionization ($p_{a\infty}$), and wall losses (p_w) into account.

The fluid model is based on the first moments of the kinetic Boltzmann equation, which result in balances for the particle, momentum, and energy densities. At not too low pressures the inelastic processes can be accounted for by rate coefficients that depend on the local value of the reduced electric field E/p_0. E and p_0 are the magnitude of the field strength and the gas pressure, respectively, i.e., the functional dependences of the coefficients on the reduced field are supposed to be the same as at equilibrium. The transport coefficients are further input data and can also be calculated as functions of the reduced electric field. Since in the static and homogeneous case the mean electron energy U_{em} is an increasing function of E/p_0, all the mentioned coefficients can be expressed as functions of U_{em}. A detailed discussion of the different ways of estimating the various coefficients is given in the paper of Boeuf and Pitchford [28]. If the system of equations is supplemented by Maxwell's equations describing the quasistatic electric field

$$\varepsilon_0 \mathrm{div} \vec{E} = e(n_i - n_e), \quad \mathrm{rot} \vec{E} = \vec{0}, \tag{2.13}$$

we obtain a complete set of equations for the variables $n_e, n_i, n_m, U_{em}, \vec{E}$.

To make the set of equations analytically tractable some physically motivated simplifying assumptions are used.

(1) In a neon discharge at low reduced field strength E/p_0 the calculation of the transport coefficients can be well approximated by using the Druyvesteyn distribution as the isotropic part of the stationary distribution function (cf. [29,30]). In this approximation there exist simple relations between the transport coefficients and the mean energy U_{em}. Introducing the temperature U_e by

$$U_{em} = \varepsilon U_e,$$

one gets

$$D_e = \alpha U_e b_e,$$

$$K_e = \beta U_e b_e,$$

$$b_e^* = \gamma b_e,$$

$$D_e^* = \alpha^* U_e b_e ,$$

$$K_e^* = \beta^* U_e b_e ,$$

with the kinetic coefficients [30]

$$\alpha = 0.842, \quad \beta = 0.281, \quad \gamma = 1.476, \quad \alpha^* = 0.956,$$

$$\beta^* = 1.275, \quad \varepsilon = 1.05. \tag{2.14}$$

The collision rates, however, cannot be well approximated by using a standard distribution function. Therefore, instead of the Druyvesteyn distribution the solution of the stationary Boltzmann equation in the spatially homogeneous case is used. This so-called conventional homogeneous approach [31] yields transport and rate coefficients that are independent of the radial position in the plasma column. Some collision rates strongly depend on E/p_0. The corresponding expressions are presented in the Appendix. Of course, the rates z_A and z_{mg} do not depend on the electron distribution function. Because in the stationary case U_{em} also depends on E/p_0, it is possible to express the collision rates as a function of U_{em} or as a function of U_e if a temperature can be defined as above. Alternatively, one can directly express the collision rates as a function of U_e if one treats as equivalent the value of the characteristic energy D_e/b_e obtained from the mentioned Boltzmann equation solution, i.e., $D_e/b_e = f(E/p_0)$ (cf. the Appendix), with the generalized Nernst-Einstein-Townsend relation $D_e/b_e = \alpha U_e$. For the calculation of the equilibrium solutions $N_0, M_0, U_{e0}, E_0, I_0$ the discussed replacement of E/p_0 by U_e in the collision rates produces only small deviations of few percent. In the following it is assumed that the collision rates used in the stationary and homogeneous case are valid in the low-frequency regime too. Although the different treatment of transport coefficients and collision rates is inconsistent, we use this way because complicated coefficients for the space derivatives in the balance equations will be avoided and the bifurcation problem becomes analytically tractable.

(2) Quasineutrality, i.e., $n_e = n_i$, in the positive column is fulfilled because the wavelength is large in comparison to the Debye length. The result is that we have only one balance equation for the density of charge carriers now denoted by n.

(3) Radial perturbations of the plasma characteristics as well as radial dependence of the stationary mean electron energy are neglected. This allows one to obtain a one-dimensional approximation by cross-section averaging, which can be performed if the radial dependences of n, m, U_e, E_x are known in the stationary and axially homogeneous case. For simplicity, we assume that the Bessel function J_0 as a function of r describes the particle densities. In fact, J_0 is an eigenfunction of the radial problem if only direct ionization acts as the sole production process. A consequent treatment would require the consideration of the boundary layer, in which quasineutrality is not realized. In the approximation used the wall recombination of electrons and ions appears as an additional loss term in the charge-carrier balance. The same assumption is used for the metastable atoms. The cross-section averaging of the energy balance produces a wall relaxation term, whose sign depends on the distribution function. In the case of a Druyvesteyn distribution this term gives an energy gain by wall recombination. This unphysical result arises from the assumption that the distribution function is independent of the radial coordinate. In the following calculations this term is neglected.

(4) The time derivative in the energy balance is neglected. It is easy to see that this is possible because the electron mobility b_e is very large in comparison to the ion mobility b_i.

(5) The diffusion of metastable atoms along the axis is neglected. This assumption considerably reduces the amount of calculation, i.e., the balance equation for metastable atoms becomes an ordinary differential equation. This neglect is not motivated by experiments. One can show that the diffusion term has a remarkable influence on the stability borders and frequencies of waves [32]. In subsequent calculations, which should improve the quantitative agreement with the experiments, we hope that we can master this term.

(6) The outer circuit, which consists of an external voltage U and an external resistance R_a, is taken into account by Kirchhoff's rule

$$U = R_a I + \int_0^L E_x dx. \tag{2.15}$$

I is the discharge current and the integral determines the voltage across the positive column. This means that I has to be considered as an additional variable, which depends only on t. The set of equations becomes a system of integro-differential equations.

By considering (2) and (3) with the averaging assumptions

$$n = n(r,x,t) = N(x,t)\frac{g(r)}{\overline{g}},$$

$$m = m(r,x,t) = M(x,t)\frac{h(r)}{\overline{h}},$$

$$j_r = 0,$$

$$j_x = j_x(r,t) = \frac{I(t)}{\pi r_0^2}\frac{g(r)}{\overline{g}}, \tag{2.16}$$

$$U_e = U_e(x,t),$$

$$E_x = E_x(x,t),$$

where

$$g(r) = h(r) = J_0\left(\lambda_1 \frac{r}{r_0}\right),$$

$$\overline{g} = \frac{2}{r_0^2}\int_0^{r_0} g(r) r \, dr,$$

$$\overline{h} = \frac{2}{r_0^2}\int_0^{r_0} h(r) r \, dr,$$

one gets the set

$$\frac{\partial N}{\partial t}=(\alpha+\beta)b_i\frac{\partial U_e}{\partial x}\frac{\partial N}{\partial x}+b_i\left(\alpha U_e\frac{\partial^2 N}{\partial x^2}+\beta N\frac{\partial^2 U_e}{\partial x^2}\right)-\frac{\lambda_1^2}{r_0^2}b_i\alpha U_e N+\overline{P}, \tag{2.17}$$

$$\frac{\partial M}{\partial t}=D_m\frac{\partial^2 M}{\partial x^2}-\frac{\lambda_1^2}{r_0^2}D_m M+\overline{P_m}, \tag{2.18}$$

$$\frac{\partial(\varepsilon N U_e)}{\partial t}=-\varepsilon b_e\left\{(\gamma\alpha-\alpha^*)\left(U_e^2\frac{\partial^2 N}{\partial x^2}-\frac{\lambda_1^2}{r_0^2}NU_e^2\right)+(\gamma\beta-\beta^*)N\left[U_e\frac{\partial^2 U_e}{\partial x^2}+\left(\frac{\partial U_e}{\partial x}\right)^2\right]+[2(\gamma\alpha-\alpha^*)+\gamma\beta-\beta^*]U_e\frac{\partial N}{\partial x}\frac{\partial U_e}{\partial x}\right\}+\frac{I}{e\pi r_0^2}\left(E_x+\gamma\frac{\partial U_e}{\partial x}\right)-N\overline{H}, \tag{2.19}$$

$$I=e\pi r_0^2 b_e\left(NE_x+\alpha U_e\frac{\partial N}{\partial x}+\beta N\frac{\partial U_e}{\partial x}\right). \tag{2.20}$$

$\overline{P},\overline{P_m},\overline{H}$ are the averaged source terms

$$\overline{P}=z_{0\infty}n_g N+z_{m\infty}\alpha_0 NM+z_A\beta_0 M^2, \tag{2.21}$$

$$\overline{P_m}=z_{0m}n_g N-z_{mg}n_g M-z_{me}\alpha_0 NM-2z_A\beta_0 M^2, \tag{2.22}$$

$$\overline{H}=n_g(p_{el}+p_{0a}+p_{0\infty}+p_w)+p_{a\infty}\alpha_0 M. \tag{2.23}$$

α_0,β_0 are averaged quantities given by

$$\alpha_0=\frac{\overline{gh}}{\overline{g}\,\overline{h}}=\frac{\lambda_1^2}{4},$$

$$\beta_0=\frac{\overline{h^2}}{\overline{h}^2}=\frac{\lambda_1^2}{4},$$

where $\lambda_1=2.4048\ldots$ is the first zero of J_0 and r_0 is the tube radius. According to assumptions (3) and (4) in the energy balance (2.19) the terms with a time derivative and the unrealistic energy gain by radial diffusion in the following will be neglected. Also the axial diffusion term in Eq. (2.18) is omitted in further calculations. For the discussion in Sec. III the homogeneous equilibrium of the system (2.17)–(2.20) and (2.15) has to be investigated. From this set we obtain equilibrium values N_0,M_0,U_{e0},E_0,I_0 as solutions of

$$\frac{\lambda_1^2}{r_0^2}b_i\alpha U_{e0}N_0=P_0\equiv z_{0\infty}n_g N_0+z_{m\infty}\alpha_0 N_0 M_0+z_A\beta_0 M_0^2,$$

$$\frac{\lambda_1^2}{r_0^2}D_m M_0=P_{m0}\equiv z_{0m}n_g N_0-z_{mg}n_g M_0-z_{me}\alpha_0 N_0 M_0-2z_A\beta_0 M_0^2,$$

$$\frac{I_0E_0}{e\pi r_0^2 N_0}=H_0\equiv n_g(p_{el}+p_{0a}+p_{0\infty}+p_w)+\alpha_0 p_{a\infty}M_0, \tag{2.24}$$

$$I_0=\pi r_0^2 e b_e N_0 E_0,$$

$$U=R_a I_0+E_0 L.$$

According to the assumption (1), the rate coefficients are expressed as functions of U_e. In the following we investigate the stability and the bifurcations of the calculated solutions. For this reason it is advantageous to describe the system with variables that measure the deviation from the equilibrium:

$$u\equiv\frac{N-N_0}{N_0},\quad m\equiv\frac{M-M_0}{M_0},\quad v\equiv\frac{U_e-U_{e0}}{U_{e0}},$$

$$w\equiv\frac{E_x-E_0}{E_0},\quad i\equiv\frac{I-I_0}{I_0}. \tag{2.25}$$

Also the independent variables are transformed into a dimensionless form

$$\xi\equiv\frac{E_0}{U_{e0}}x,\quad \tau\equiv\frac{b_i E_0^2}{U_{e0}}t. \tag{2.26}$$

Introducing these new variables and expanding the source terms $\overline{P},\overline{P_m},\overline{H}$ up to third order in u,m,v yields the set of equations

$$\frac{\partial}{\partial\tau}(\hat{I}X)=\hat{L}X+N_2(X,X)+N_3(X,X,X)+\cdots, \tag{2.27}$$

where

$$X=\begin{pmatrix}u\\m\\v\\w\end{pmatrix},\quad \hat{I}=\begin{pmatrix}1&0&0&0\\0&1&0&0\\0&0&0&0\\0&0&0&0\end{pmatrix}. \tag{2.28}$$

The linear terms are given by

$$\hat{L}X=\begin{pmatrix}L_1u+L_2v+\eta_3 m\\ L_3m+\eta_4u+\eta_5v\\ L_4u+L_5v+i+w-h_4m\\ -i+u+w+\alpha\dfrac{\partial u}{\partial\xi}+\beta\dfrac{\partial v}{\partial\xi}\end{pmatrix}, \tag{2.29}$$

with the current perturbation

$$i=-\frac{R}{R_a}\frac{1}{l}\int_0^l w\,d\xi \quad \text{with} \quad R=\frac{E_0 L}{I_0}, \quad l=\frac{E_0}{U_{e0}}L. \tag{2.30}$$

L_1, L_2, L_3, L_4, L_5 are linear operators represented by

$$L_1 u=\alpha\frac{\partial^2 u}{\partial\xi^2}+\eta_1 u, \tag{2.31}$$

$$L_2 v=\beta\frac{\partial^2 v}{\partial\xi^2}+\eta_2 v, \tag{2.32}$$

$$L_3 m=\widetilde{D}\frac{\partial^2 m}{\partial\xi^2}+\eta_6 m, \tag{2.33}$$

$$L_4 u=-\delta_1\frac{\partial^2 u}{\partial\xi^2}-u, \tag{2.34}$$

$$L_5 v=-\delta_2\frac{\partial^2 v}{\partial\xi^2}+\varepsilon\gamma\frac{\partial v}{\partial\xi}-h_1 v. \tag{2.35}$$

For the quadratic and cubic terms we obtain

N_2

$$=\begin{pmatrix} \alpha v\dfrac{\partial^2 u}{\partial\xi^2}+(\alpha+\beta)\dfrac{\partial u}{\partial\xi}\dfrac{\partial v}{\partial\xi}+\beta u\dfrac{\partial^2 v}{\partial\xi^2} \\ +\rho_1 uv+\rho_2 v^2+\rho_3 um+\rho_4 vm+\rho_5 m^2 \\ \rho_6 uv+\rho_7 v^2+\rho_8 um+\rho_9 vm+\rho_{10} m^2 \\ -2\delta_1 v\dfrac{\partial^2 u}{\partial\xi^2}-\delta_2(u+v)\dfrac{\partial^2 v}{\partial\xi^2}-\delta_3\dfrac{\partial u}{\partial\xi}\dfrac{\partial v}{\partial\xi}-\delta_2\left(\dfrac{\partial v}{\partial\xi}\right)^2 \\ +iw+\varepsilon\gamma i\dfrac{\partial v}{\partial\xi}-h_1 uv-h_2 v^2-h_4 um-h_5 vm \\ \alpha v\dfrac{\partial u}{\partial\xi}+\beta u\dfrac{\partial v}{\partial\xi}+uw \end{pmatrix} \tag{2.36}$$

and

$$N_3=\begin{pmatrix} \sigma_0 umv+\sigma_1 uv^2+\sigma_2 v^3+\sigma_3 mv^2+\sigma_4 m^2 v \\ \sigma_5 uv^2+\sigma_6 v^3+\sigma_7 mv^2+\sigma_8 m^2 v \\ -\delta_1 v^2\dfrac{\partial^2 u}{\partial\xi^2}-\delta_2 uv\dfrac{\partial^2 v}{\partial\xi^2}-\delta_3 v\dfrac{\partial u}{\partial\xi}\dfrac{\partial v}{\partial\xi}-\delta_2 u\left(\dfrac{\partial v}{\partial\xi}\right)^2 \\ -h_2 uv^2-h_3 v^3-h_5 uvm-h_6 v^2 m \\ 0 \end{pmatrix}, \tag{2.37}$$

respectively, where

$$\delta_1=\varepsilon(\gamma\alpha-\alpha^*), \quad \delta_2=\varepsilon(\gamma\beta-\beta^*), \quad \delta_3=2\delta_1+\delta_2, \tag{2.38}$$

and

$$\widetilde{D}=\frac{D_m}{b_i U_{e0}}. \tag{2.39}$$

This set of equations has to be supplemented by boundary conditions at the ends of the positive column. According to Landa [25], we use Dirichlet boundary conditions

$$\begin{aligned} u(0)&=u(l)=0, \\ m(0)&=m(l)=0, \\ v(0)&=v(l)=0. \end{aligned} \tag{2.40}$$

The calculated spatial damping of the eigenfunctions, which lower their amplitudes going from the anode to the cathode (cf. Sec. III), yields an *a posteriori* justification because the same spatial behavior is observed in experiments. In conformity with assumption (5), we neglect the axial diffusion of metastable atoms, i.e., we set $\widetilde{D}=0$. In this case the vanishing of m at the boundaries is fulfilled automatically. Those coefficients in Eqs. (2.29) and (2.31)–(2.37) that are not defined in this section are given in the Appendix. The various $\eta_i, \sigma_j, \rho_k, h_l$ are the coefficients in the Taylor series of the averaged source terms $\overline{P}, \overline{P_m}, \overline{H}$. Note that they depend on the equilibrium state, i.e., they can be calculated as functions of I_0.

III. LINEAR STABILITY

In the following we study the bifurcations of the equilibrium state. Therefore, first of all, the stability of this solution and its parameter dependence have to be investigated by discussing the eigenvalue problem

$$\hat{L}X_{10}=p\hat{I}X_{10}. \tag{3.1}$$

p denotes the complex eigenvalue belonging to the vector eigenfunction

$$X_{10}=\begin{pmatrix} u_{10} \\ m_{10} \\ v_{10} \\ w_{10} \end{pmatrix}. \tag{3.2}$$

Also the complex conjugate p^* is an eigenvalue with the eigenfunction $X_{01}=X_{10}^*$. The ansatz $X_{10}=C\exp(q\xi)+C_0$ with complex constants C, C_0 generates the dispersion relation

$$\begin{vmatrix} \alpha q^2+\eta_1-p & \eta_3 & \beta q^2+\eta_2 & 0 \\ \eta_4 & \eta_6-p & \eta_5 & 0 \\ -\delta_1 q^2-1 & -h_4 & -\delta_2 q^2+\varepsilon\gamma q-h_1 & 1 \\ 1+\alpha q & 0 & \beta q & 1 \end{vmatrix}=0. \tag{3.3}$$

Equation (3.3) connects the complex eigenvalue $p=\mu+i\omega$ with the complex q. For a given p there are four values of q. This enables us to construct the components of the eigenvector:

$$u_{10}=\sum_{j=1}^{4}[\exp(q_j\xi)+U_0K_j]C_j,\qquad v_{10}=\sum_{j=1}^{4}[V_j\exp(q_j\xi)+V_0K_j]C_j,$$

$$m_{10}=\sum_{j=1}^{4}[M_j\exp(q_j\xi)+M_0K_j]C_j,\qquad w_{10}=\sum_{j=1}^{4}[W_j\exp(q_j\xi)+W_0K_j]C_j, \tag{3.4}$$

where

$$U_0=\frac{1}{F\dfrac{R+R_a}{2R}-1},\quad V_0=U_0\frac{(p-\eta_1)(p-\eta_6)-\eta_3\eta_4}{\eta_2(p-\eta_6)+\eta_3\eta_5},\quad M_0=U_0\frac{\eta_5(p-\eta_1)+\eta_2\eta_4}{\eta_2(p-\eta_6)+\eta_3\eta_5},\quad W_0=\frac{R-R_aU_0}{R+R_a},$$

$$V_j=\frac{\eta_3(\delta_1q_j^2+\alpha q_j+2)+h_4(p-\alpha q_j^2-\eta_1)}{-\eta_3(\delta_2q_j^2-\delta_4q_j+h_1)+h_4(\beta q_j^2+\eta_2)},\quad M_j=\frac{\eta_4+\eta_5V_j}{p-\eta_6},\quad W_j=-1-(\alpha+\beta V_j)q_j,\quad K_j=\frac{\exp(q_jl)-1}{q_jl},$$

$$F=\frac{(p-\eta_6)(h_1(p-\eta_1)+2\eta_2)+\eta_3(2\eta_5-h_1\eta_4)+h_4(\eta_5(p-\eta_1)+\eta_2\eta_4)}{\eta_2(p-\eta_6)+\eta_3\eta_5},$$

and $\delta_4=\varepsilon\gamma-\beta$.

The complex C_j $(j=1,2,3,4)$ will be determined by the boundary conditions (2.40). The solvability condition for the homogeneous system gives the secular equation

$$D\equiv\begin{vmatrix}1+U_0K_1 & 1+U_0K_2 & 1+U_0K_3 & 1+U_0K_4\\ e^{q_1l}+U_0K_1 & e^{q_2l}+U_0K_2 & e^{q_3l}+U_0K_3 & e^{q_4l}+U_0K_4\\ V_1+V_0K_1 & V_2+V_0K_2 & V_3+V_0K_3 & V_4+V_0K_4\\ V_1e^{q_1l}+V_0K_1 & V_2e^{q_2l}+V_0K_2 & V_3e^{q_3l}+V_0K_3 & V_4e^{q_4l}+V_0K_4\end{vmatrix}=0. \tag{3.5}$$

This equation together with Eq. (3.3) fixes the eigenvalues of Eq. (3.1), which, in general, can only be calculated by numerical methods. For the stability investigations the following situation is of particular importance: few eigenvalues have a vanishing real part, whereas the remaining discrete set posseses negative real parts. Graphical methods can be helpful in realizing this situation. Choosing a path along the imaginary axis while going from $-\infty$ to $+\infty$ and closing this path in the right half plane, the corresponding curve in the D plane leaves the origin on the left-hand side if no eigenvalue with a positive real part exists. Varying the parameters, one can find situations where the curve in the D plane passes through the origin. For accurate quantitative results root finding methods have to be used. In this manner the stability diagram of Fig. 1 is found, where the length of the positive column L and the equilibrium current I_0 are considered as parameters. The neutral gas pressure p_0 and the tube radius r_0 are held constant. We have chosen $p_0=200$ Pa and $r_0=1$ cm. The represented curves are the loci of those points, which possess one eigenvalue with a vanishing real part, i.e., these curves mark codimension-one bifurcations. At the crossing points of two curves there are codimension-two bifurcations. The stable side is at lower currents. The bifurcations describe the formation of low-frequency ionization waves (so-called p waves). An example of an eigenfunction set $X_{10}^T=(u_{10},v_{10},m_{10},w_{10})$ at the stability boundary is shown in Fig. 2. Going from the anode (left) to the cathode (right) the amplitudes of the components diminish. This is in accordance with the experimental observations [7]. Furthermore, one observes phase shifts between the components. These shifts are responsible for the direction of phase veloc-

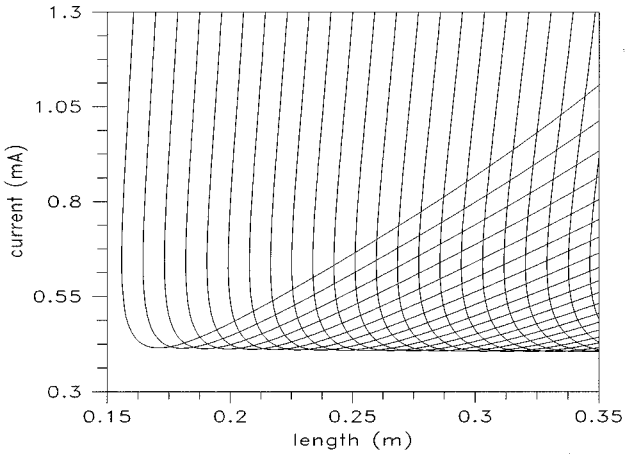

FIG. 1. Stability boundaries in parameter space of the modes 18–40. Additional parameters are $R_a=10^5$ Ω, $r_0=1.0$ cm, and $p_0=200$ Pa.

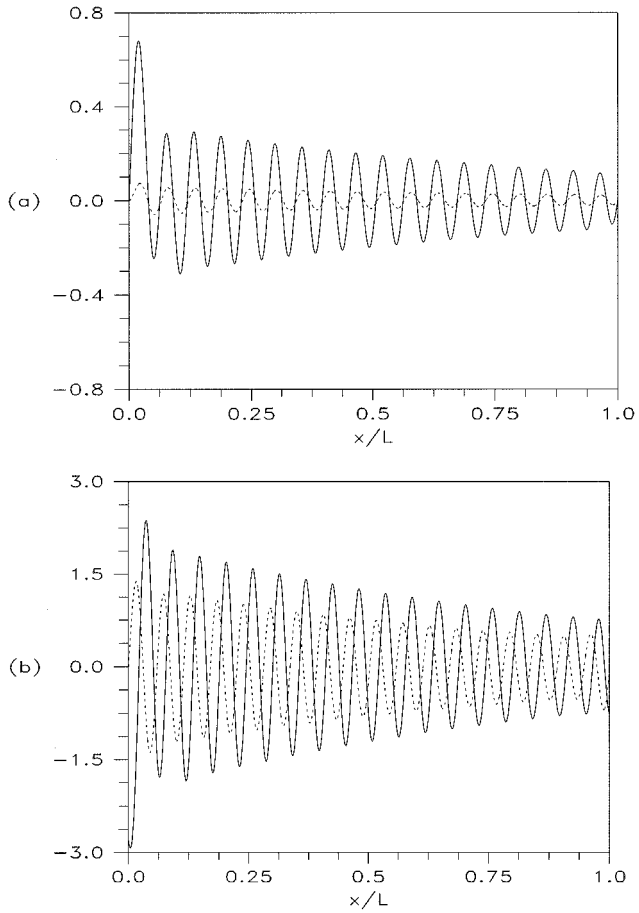

FIG. 2. Real parts of the components of the eigenfunction X_{10} at the stability boundary of mode $J=18$. The parameters are $R_a=10^5\ \Omega$, $I_0=0.415$ mA, $L=0.171$ m, and the calculated eigenfrequency $f=138\ \mathrm{s}^{-1}$. (a) Full line, Re(u_{10}); dashed line, Re(v_{10}). (b) Full line, Re(w_{10}); dashed line, Re(m_{10}).

ity and the mechanism of instability. A temperature rise is followed by an additional production of charge carriers, i.e., if there is a positive phase shift of the temperature relative to the charge density, the wave moves to the cathode. If there is only a small phase shift between the densities of charge carriers and metastable atoms, the instability develops. Although the eigenfunctions (3.4) are the sum of four partial waves, only one dominates. Therefore, a mode number J can be defined as the number of maxima (or minima). Likewise, a mean wavelength λ can be calculated as $\lambda=L/J$. At very low currents a second instability is found, which is characterized by higher frequencies and lower wavelengths. We plan to study these so-called r waves in a subsequent paper.

In the calculations of Sec. IV the solution of the adjoint problem

$$\hat{L}^{\dagger}Y_{10}=p^{*}\hat{I}Y_{10} \quad \text{with} \quad Y_{10}=\begin{pmatrix}\tilde{u}_{10}\\ \tilde{v}_{10}\\ \tilde{m}_{10}\\ \tilde{w}_{10}\end{pmatrix} \tag{3.6}$$

is also needed. As usual, the adjoint $\hat{L}^{\dagger}$ of the linear operator $\hat{L}$ is defined by the scalar product

$$\langle X|\hat{L}Y\rangle=\langle\hat{L}^{\dagger}X|Y\rangle, \tag{3.7}$$

where the L_2 scalar product

$$\langle X|Y\rangle=\int_0^l X^{\dagger}Y\,d\xi \tag{3.8}$$

is taken with four-dimensional vectors. $X^{\dagger}$ is the transposed of the complex conjugate. Now it is a simple task to calculate the eigenfunctions of $L^{\dagger}$. One obtains

$$\begin{aligned}
\tilde{u}_{10}&=\sum_{j=1}^{4}[\exp(-q_j^{*}\xi)+\tilde{U}_0\tilde{K}_j]\tilde{C}_j,\\
\tilde{m}_{10}&=\sum_{j=1}^{4}[\tilde{M}_j\exp(-q_j^{*}\xi)+\tilde{M}_0\tilde{K}_j]\tilde{C}_j,\\
\tilde{v}_{10}&=\sum_{j=1}^{4}[\tilde{V}_j\exp(-q_j^{*}\xi)+\tilde{V}_0\tilde{K}_j]\tilde{C}_j,\\
\tilde{w}_{10}&=\sum_{j=1}^{4}[\tilde{W}_j\exp(-q_j^{*}\xi)+\tilde{W}_0\tilde{K}_j]\tilde{C}_j,
\end{aligned} \tag{3.9}$$

where

$$\tilde{U}_0=U_0^{*},$$

$$\tilde{V}_0=\tilde{U}_0\frac{\eta_3\eta_5+\eta_2(p^{*}-\eta_6)}{\eta_5h_4+h_1(p^{*}-\eta_6)},$$

$$\tilde{M}_0=\tilde{U}_0\frac{\eta_3h_1-\eta_2h_4}{\eta_5h_4+h_1(p^{*}-\eta_6)},$$

$$\tilde{W}_0=\frac{\tilde{V}_0}{\tilde{U}_0}\frac{2R+(R-R_a)\tilde{U}_0}{R+R_a},$$

$$\tilde{V}_j=\frac{\eta_4(\beta q_j^{*2}+\eta_2)+\eta_5(p^{*}-\alpha q_j^{*2}-\eta_1)}{\eta_4(\delta_2q_j^{*2}-\delta_4q_j^{*}+h_1)-\eta_5(\delta_1q_j^{*2}+\alpha q_j^{*}+2)},$$

$$\tilde{M}_j=\frac{\eta_3-h_4\tilde{V}_j}{p^{*}-\eta_6},$$

$$\tilde{W}_j=-\tilde{V}_j,$$

$$\tilde{K}_j=-\tilde{V}_j\frac{\tilde{U}_0}{\tilde{V}_0}\frac{\exp(-q_j^{*}l)-1}{q_j^{*}l}.$$

IV. CENTER MANIFOLD REDUCTION

To discuss the various bifurcations of the homogeneous state the basic system has to be reduced to the corresponding normal form equation. This reduction is only valid for sufficiently small deviations from the equilibrium solution. Center manifold reduction and transformation to the normal form will be performed in one step [33]. In the case of single Hopf

bifurcations the local dynamics can be described by the normal form equation, which up to third order is given by

$$\dot{z}=pz+A|z|^2z+\cdots. \tag{4.1}$$

The complex eigenvalue p, which has been calculated in Sec. II, and the third-order nonlinearity constant A depend on the parameters of the system. The calculation of A is the main task in this section. In the case of $\mathrm{Re}(A)<0$ $[\mathrm{Re}(A)>0]$ the Hopf bifurcation is supercritical (subcritical), i.e., a limit cycle arises on the side where the homogeneous solution is unstable (stable) in parameter space. This limit cycle is stable only in the case of supercritical Hopf bifurcations at the first instability. $\mathrm{Re}(A)=0$ marks a generalized Hopf bifurcation, where a fifth-order term in the normal form of Eq. (4.1) has to be added to unfold this singularity. This codimension-two bifurcation is planned to be discussed in a subsequent paper. For the time-dependent state vector X on the center manifold, which is tangential to the center subspace, we make the following ansatz up to order n:

$$X(\xi,\tau)=\sum_{i+j=1}^{i+j=n} X_{ij}(\xi)z^i(\tau)z^{*j}(\tau) \quad \text{with} \quad X_{ij}=X_{ji}^*. \tag{4.2}$$

$X_{10}(\xi),X_{01}(\xi)$ are the linear eigenvectors (eigenfunctions), which span the center subspace. $X_{ij}(\xi)$ with $i+j>1$ describe the deviation of the nonlinear center manifold from the linear center subspace. The center space coordinate $z(\tau)$ characterizes the motion on the center manifold. With a view to investigate Hopf bifurcations we claim that $z(\tau)$ fulfills Eq. (4.1). To calculate A we insert the expansion (4.2) into Eq. (2.27). Comparing the coefficients of the terms with z^iz^{*j} gives a sequence of linear systems of ascending order. To first order $(i+j=1)$ we obtain the eigenvalue equation (3.1) and its conjugate complex, which both were solved at the stability boundary of the different modes in Sec. II. To second order $(i+j=2)$ three sets of equations have to be solved:

$$(\hat{L}-2i\omega)X_{20}=-N_2(X_{10},X_{10}), \tag{4.3a}$$

$$\hat{L}X_{11}=-N_2(X_{10},X_{01}), \tag{4.3b}$$

$$(\hat{L}+2i\omega)X_{02}=-N_2(X_{01},X_{01}). \tag{4.3c}$$

The inhomogeneities on the right-hand side consist of eigenfunctions and their derivatives, which must be inserted in the quadratic terms of N_2 [cf. Eq. (2.36)]. The second-order functions X_{20},X_{11},X_{02} have to fulfill the boundary conditions (2.40). Furthermore, we have $X_{02}=X_{20}^*$ and $X_{11}=X_{11}^*$. In general, $2i\omega$ and 0, respectively, are not eigenvalues of the linear operator $\hat{L}$. In this case the inhomogeneous systems (4.3) have unique solutions, which can be found by numerical calculations or as we have done by analytical methods. A special solution of Eq. (4.3a) may be found by the ansatz

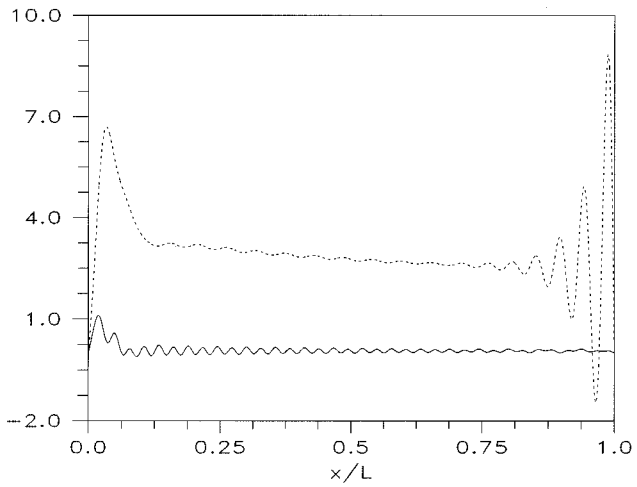

FIG. 3. Second-order corrections of the charge-carrier density. Full line, $\mathrm{Re}(u_{20})$; dashed line, u_{11}. The parameters are the same as in Fig. 2.

$$X_{20}=\sum_{i,j=1}^{4} A_{ij}\exp[(q_i+q_j)\xi]+\sum_{i=1}^{4} A_i\exp(q_i\xi)+A_0. \tag{4.4}$$

With a similar ansatz one obtains a special solution of Eq. (4.3b) Generally, these functions do not satisfy the boundary conditions. Therefore, a special solution of the homogeneous problem has to be added to obtain the desired solution. An example of the second-order corrections u_{20},u_{11} is shown in Fig. 3.

To third order $(i+j=3)$ there exist four inhomogeneous systems referring to the coefficients of $z^3,z^2z^*,zz^{*2},z^{*3}$. To calculate the Hopf parameter A only the system corresponding to z^2z^* has to be discussed [cf. Eq. (4.1)]. This set of linear equations has the structure

$$(\hat{L}-i\omega)X_{21}=A\hat{I}X_{10}-N_2(X_{20},X_{01})-N_2(X_{11},X_{10}) -N_3(X_{10},X_{10},X_{01}). \tag{4.5}$$

The first term of the inhomogeneity includes the constant A. Furthermore, there are quadratic and cubic terms. The quadratic ones consist of eigenfunctions and second-order functions and their derivatives in the combinations indicated as arguments of N_2. The cubic term contains only eigenfunctions and their derivatives. The explicit form of these terms is not given here. It is simple but tedious to write down all the terms needed. Apparently, the eigenvector X_{10} is the unique solution of the homogeneous set. Therefore, the second part of the Fredholm alternative plays a role, i.e., the inhomogeneity has to be orthogonal with respect to the eigenvector Y_{10} of the adjoint problem. This condition determines the value of A by

$$A=\frac{\int_0^l Y_{10}^{\dagger}[N_2(X_{20},X_{01})+N_2(X_{11},X_{10})+N_3(X_{10},X_{10},X_{01})]d\xi}{\int_0^l Y_{10}^{\dagger}\hat{I}X_{10}d\xi}. \tag{4.6}$$

The detailed formula, which shows precisely the dependence of A on all system parameters, actually represents the main result of this paper. It is too involved to be shown here. Instead of this, the graphic representation of Eq. (4.6) will be given in Sec. V. The eigenvector X_{10} contains an arbitrary complex constant K, which also appears in the second-order corrections X_{20},X_{11},X_{02} as K^2,KK^*,K^{*2}. According to Eq. (4.6), A includes a factor KK^* too. Therefore, the solution $z(\tau)$ of the normal form of Eq. (4.1) comprises the factor $1/K$, i.e., the constant K can be eliminated by replacing $z\rightarrow z/K$. Following these arguments one sees that the state vector X [cf. Eq. (4.2)] is independent of K as it must be.

The validity of the results obtained in this section is essentially based on the existence of the center manifold near the origin of the system (2.27). Until now there has been no strong proof, but we hope that we can close this gap in our argumentation.

V. RESULTS AND DISCUSSION

First of all, the quantitative outcomes of the linear theory should be compared with experimental results. We have found the minima of the stability boundaries at about 0.4 mA with a weak dependence on the mode number and the external resistance R_a. At these minima the wavelength and frequency are given approximately by $\lambda=0.95$ cm and $f=140\ \mathrm{s}^{-1}$, respectively. On the right branch of the instability curves our results are closer to the experimental values $\lambda\approx 2.9$ cm and $f\approx 600\ \mathrm{s}^{-1}$ ($p_0=227$ Pa, $R_a=10^5\ \Omega$) [8,35]. The experimental instability region begins at $I_0=3.5$ mA for $R_a=10^5\ \Omega$ and at $I_0=6.2$ mA for $R_a=10^6\ \Omega$ [35]. If the diffusion of metastable atoms is taken into account, the linear calculations approximate essentially better to the experimental results [32]. A correct comparison demands the consideration of nonlinear results, i.e., the calculation of the complete regions, where stable traveling waves are possible.

For given parameter values p_0,r_0,R_a the constant A in Eq. (4.1) can be calculated at the stability boundary, which is marked by a characteristic curve $I_0=I_0(L)$ for a given mode. The sign of the real part of A determines the type of the Hopf bifurcation. Figures 4 and 5 show the results for two different values of the resistance of the outer circuit. Whereas the position of the border of stability has only a weak dependence on R_a, the type of Hopf bifurcation at a given parameter set may be changed. The bifurcations at the first instability are the most interesting ones because they should be observable in real or numerical experiments. For $R_a=10^4\ \Omega$ at the boundary only supercritical bifurcations are observed, whereas for $R_a=10^5\ \Omega$ there are both types of bifurcations. This statement is valid only for the modes represented. At higher R_a the same phenomena will be observed at larger L. This can be approximately estimated by the discussion of the current perturbation $i=-E_0/(R_aI_0)\int_0^L w\ dx$. In this expression larger values of R_a can be compensated by a longer integration length L.

Going at fixed length to larger values of the current, additional modes are generated, but even if the Hopf bifurcation is supercritical the developing limit cycle has some unstable directions, i.e., it is unstable. We speculate that there must be subcritical bifurcations, which stabilize some of the cycles, so that one or two (or more) are observable in experiments. Such results were obtained by Tuckerman and Barkley [34] in the case of stationary solutions of the real Ginzburg-Landau equation. Experimental investigations in

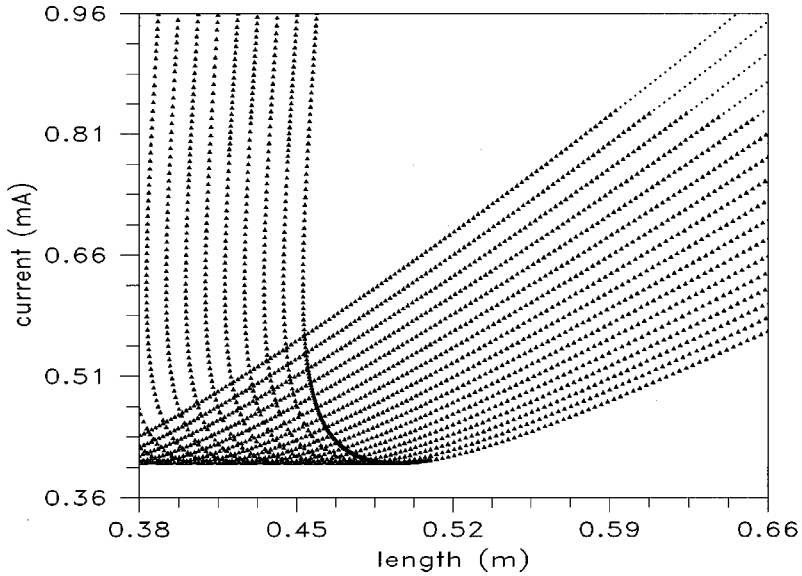

FIG. 4. Supercritical (triangles) and subcritical (dots) Hopf bifurcations, respectively, at the stability boundaries of the modes 36–52. The parameters are $R_a=10^4\ \Omega$, $r_0=1.0$ cm, and $p_0=200$ Pa.

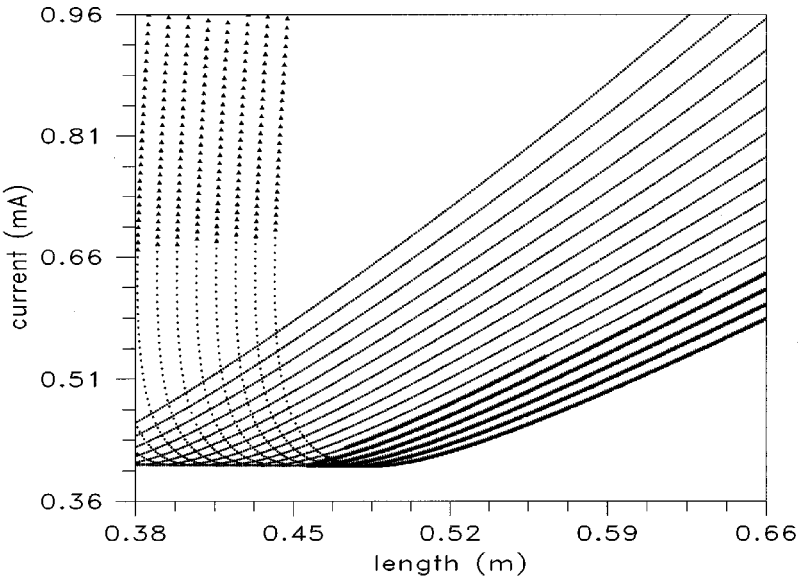

FIG. 5. Supercritical (triangles) and subcritical (dots) Hopf bifurcations, respectively, at the stability boundaries of the modes 36–52. The parameters are $R_a = 10^5\ \Omega$, $r_0 = 1.0$ cm, and $p_0 = 200$ Pa.

neon show a strong pattern selection [36], i.e., within the Eckhaus region only one or two modes are stable. This is a considerable difference from the classical Eckhaus results, where a band of modes is stable at a given parameter set.

There are not only supercritical and subcritical bifurcations but also transitions from one type to the other on a given bifurcation curve. This codimension-two bifurcation is a generalized Hopf bifurcation. The unfolding of this singularity yields a stable and an unstable limit cycle on the center manifold. But to do this a fifth-order term $B|z|^4 z$ has to be supplemented in Eq. (4.1). Furthermore, crossings of mode curves of three different types are observed: there are super-super, sub-sub, and super-sub crossings. For $R_a = 10^5\ \Omega$ these phenomena are situated at the stability boundary, i.e., they should be observable in experiments. To unfold these codimension-two bifurcations the calculation of further coefficients in the normal form

$$\dot{z}_1 = p_1 z_1 + A_1 |z_1|^2 z_1 + B_1 |z_1|^2 z_2 + \cdots,$$

$$\dot{z}_2 = p_2 z_2 + A_2 |z_2|^2 z_2 + B_2 |z_2|^2 z_1 + \cdots$$

is needed. Possibly, fifth-order terms have to be included. Using periodic boundary conditions, we managed to unfold this codimension-two singularity in most cases [32].

The results discussed in this paper are only a first step for the description of the pattern formation in a neon glow discharge. To obtain a better knowledge of the main bifurcations further comprehensive investigations are necessary. Codimension-two bifurcations, especially at the stability boundary, should be discussed to understand the various possibilities of passing from stable to unstable regions. In the limit of large length an approximation by means of model equations of Ginzburg-Landau type should make it possible to go some steps into the instability region and to find and understand mild forms of turbulent motions. Numerical calculations with the full set of equations and with Ginzburg-Landau equations are well on the way to completing the obtained results. Furthermore, we hope that our calculations will stimulate experimenters to search for supercritical and subcritical bifurcations and in a second step for the more complicated phenomena connected with codimension-two bifurcations.

ACKNOWLEDGMENTS

We are indebted to Dr. C. Wilke and Professor H. Deutsch for valuable discussions regarding the physics of ionization waves. The authors thank H. Leyh for calculating the stability boundaries of Fig. 1. This work has been supported by the Deutsche Forschungsgemeinschaft through ''Sonderforschungsbereich 198: Kinetik Partiell Ionisierter Plasmen.''

APPENDIX

The following collision rates and transport coefficients for a low-pressure neon discharge have been tabulated by Mönke [37] and Franke [38]:

$$z_{0\infty} = 6.930 \times 10^{-5} \left(\frac{E}{p_0} \right)^{5.3694} \text{cm}^3\ \text{s}^{-1},$$

$$z_{m\infty} = 1.346 \times 10^{-7} \left(\frac{E}{p_0} \right)^{0.0693} \text{cm}^3\ \text{s}^{-1},$$

$$z_A = 3.4 \times 10^{-10}\ \text{cm}^3\ \text{s}^{-1},$$

$$z_{0m} = 5.294 \times 10^{-13}\ \text{cm}^3\ \text{s}^{-1},$$

$$z_{mg} = 3.86 \times 10^{-15}\ \text{cm}^3\ \text{s}^{-1},$$

$$z_{me} = 2.5 \times 10^{-7}\ \text{cm}^3\ \text{s}^{-1},$$

$$\frac{D_e}{b_e} = 6.6574 \times \left(\frac{E}{p_0}\right)^{0.0751} \text{V},$$

$$p_{el} = 3.4413 \times 10^{-11} \left(\frac{E}{p_0}\right)^{0.184} \text{V cm}^3\ \text{s}^{-1},$$

$$p_{0a} = 1.083 \times 10^{-6} \left(\frac{E}{p_0}\right)^{2.1998} \text{V cm}^3\ \text{s}^{-1},$$

$$p_{0\infty} = 1.454 \times 10^{2} \left(\frac{E}{p_0}\right)^{8.824} \text{V cm}^3\ \text{s}^{-1},$$

$$p_{w} = 4.362 \times 10^{2} \left(\frac{E}{p_0}\right)^{8.912} \text{V cm}^3\ \text{s}^{-1},$$

$$p_{a\infty} = 6.6335 \times 10^{-7} \left(\frac{E}{p_0}\right)^{0.0693} \text{V cm}^3\ \text{s}^{-1},$$

$$b_e = 8.333 \times 10^{5}\ \text{cm}^2\ \text{V}^{-1}\ \text{s}^{-1},$$

$$b_i = 2.077 \times 10^{3}\ \text{cm}^2\ \text{V}^{-1}\ \text{s}^{-1},$$

$$D_m = 96.32\ \text{cm}^2\ \text{s}^{-1}.$$

To obtain the coefficients and rates in the announced units the field strength E has to be inserted in V/cm and the gas pressure p_0 in units of Pascal (Pa).

Here we give the definitions of the coefficients that have been introduced in Eqs. (2.29) and (2.31)–(2.37):

$$\eta_1 = \alpha\kappa\left(\frac{N_0}{P_0}\left.\frac{\partial\overline{P}}{\partial N}\right|_0 - 1\right),$$

$$\eta_2 = \alpha\kappa\left(\frac{U_{e0}}{P_0}\left.\frac{\partial\overline{P}}{\partial U_e}\right|_0 - 1\right),$$

$$\eta_3 = \alpha\kappa\frac{M_0}{P_0}\left.\frac{\partial\overline{P}}{\partial M}\right|_0,$$

$$\eta_4 = \kappa\tilde{D}\frac{N_0}{P_{m0}}\left.\frac{\partial\overline{P_m}}{\partial N}\right|_0,$$

$$\eta_5 = \kappa\tilde{D}\frac{U_{e0}}{P_{m0}}\left.\frac{\partial\overline{P_m}}{\partial U_e}\right|_0,$$

$$\eta_6 = \kappa\tilde{D}\left(\frac{M_0}{P_{m0}}\left.\frac{\partial\overline{P_m}}{\partial M}\right|_0 - 1\right),$$

$$\rho_1 = \alpha\kappa\left(\frac{N_0U_{e0}}{P_0}\left.\frac{\partial^2\overline{P}}{\partial N\partial U_e}\right|_0 - 1\right),$$

$$\rho_2 = \alpha\kappa\frac{U_{e0}^2}{2P_0}\left.\frac{\partial^2\overline{P}}{\partial U_e^2}\right|_0,$$

$$\rho_3 = \alpha\kappa\frac{N_0M_0}{P_0}\left.\frac{\partial^2\overline{P}}{\partial N\partial M}\right|_0,$$

$$\rho_4 = \alpha\kappa\frac{M_0U_{e0}}{P_0}\left.\frac{\partial^2\overline{P}}{\partial M\partial U_e}\right|_0,$$

$$\rho_5 = \alpha\kappa\frac{M_0^2}{2P_0}\left.\frac{\partial^2\overline{P}}{\partial M^2}\right|_0,$$

$$\rho_6 = \kappa\tilde{D}\frac{N_0U_{e0}}{P_{m0}}\left.\frac{\partial^2\overline{P_m}}{\partial N\partial U_e}\right|_0,$$

$$\rho_7 = \kappa\tilde{D}\frac{U_{e0}^2}{2P_{m0}}\left.\frac{\partial^2\overline{P_m}}{\partial U_e^2}\right|_0,$$

$$\rho_8 = \kappa\tilde{D}\frac{N_0M_0}{P_{m0}}\left.\frac{\partial^2\overline{P_m}}{\partial N\partial M}\right|_0,$$

$$\rho_9 = \kappa\tilde{D}\frac{M_0U_{e0}}{P_{m0}}\left.\frac{\partial^2\overline{P_m}}{\partial M\partial U_e}\right|_0,$$

$$\rho_{10} = \kappa\tilde{D}\frac{M_0^2}{2P_{m0}}\left.\frac{\partial^2\overline{P_m}}{\partial M^2}\right|_0,$$

$$\sigma_0 = \alpha\kappa\frac{N_0M_0U_{e0}}{P_0}\left.\frac{\partial^3\overline{P}}{\partial N\partial M\partial U_e}\right|_0,$$

$$\sigma_1 = \alpha\kappa\frac{N_0U_{e0}^2}{2P_0}\left.\frac{\partial^3\overline{P}}{\partial N\partial U_e^2}\right|_0,$$

$$\sigma_2 = \alpha\kappa\frac{U_{e0}^3}{6P_0}\left.\frac{\partial^3\overline{P}}{\partial U_e^3}\right|_0,$$

$$\sigma_3 = \alpha\kappa\frac{M_0U_{e0}^2}{2P_0}\left.\frac{\partial^3\overline{P}}{\partial M\partial U_e^2}\right|_0,$$

$$\sigma_4 = \alpha\kappa\frac{M_0^2U_{e0}}{2P_0}\left.\frac{\partial^3\overline{P}}{\partial M^2\partial U_e}\right|_0,$$

$$\sigma_5 = \kappa\tilde{D}\frac{N_0U_{e0}^2}{2P_{m0}}\left.\frac{\partial^3\overline{P_m}}{\partial N\partial U_e^2}\right|_0,$$

$$\sigma_6 = \kappa\tilde{D}\frac{U_{e0}^3}{6P_{m0}}\left.\frac{\partial^3\overline{P_m}}{\partial U_e^3}\right|_0,$$

$$\sigma_7 = \kappa\tilde{D}\frac{M_0U_{e0}^2}{2P_{m0}}\left.\frac{\partial^3\overline{P_m}}{\partial M\partial U_e^2}\right|_0,$$

$$\sigma_8=\kappa\tilde{D}\frac{M_0^2U_{e0}}{2P_{m0}}\left.\frac{\partial^3\overline{P_m}}{\partial M^2\partial U_e}\right|_0,$$

$$h_1=\frac{U_{e0}}{H_0}\left.\frac{\partial\overline{H}}{\partial U_e}\right|_0,$$

$$h_2=\frac{U_{e0}^2}{2H_0}\left.\frac{\partial^2\overline{H}}{\partial U_e^2}\right|_0,$$

$$h_3=\frac{U_{e0}^3}{6H_0}\left.\frac{\partial^3\overline{H}}{\partial U_e^3}\right|_0,$$

$$h_4=\frac{M_0}{H_0}\left.\frac{\partial\overline{H}}{\partial M}\right|_0,$$

$$h_5=\frac{M_0U_{e0}}{H_0}\left.\frac{\partial^2\overline{H}}{\partial M\partial U_e}\right|_0,$$

$$h_6=\frac{M_0U_{e0}^2}{2H_0}\left.\frac{\partial^3\overline{H}}{\partial M\partial U_e^2}\right|_0,$$

where

$$\kappa=\frac{\lambda_1^2}{r_0^2}\frac{U_{e0}^2}{E_0^2}.$$

The derivatives of the averaged source terms $\overline{P,P_m},\overline{H}$ are to be calculated at equilibrium.

[1] M.C. Cross and P.C. Hohenberg, Rev. Mod. Phys. **65**, 851 (1993).
[2] P. Manneville, *Dissipative Structures and Weak Turbulence* (Academic, New York, 1990).
[3] Y.P. Raizer, *Gas Discharge Physics* (Springer, Berlin, 1991).
[4] A.V. Nedospasov, Usp. Fiz. Nauk **94**, 439 (1968) [Sov. Phys. Usp. **11**, 174 (1968)].
[5] L. Pekarek, Usp. Fiz. Nauk **94**, 463 (1968) [Sov. Phys. Usp. **11**, 188 (1968)].
[6] N.L. Oleson and A.W. Cooper, Adv. Electron. Electron Phys. **24**, 155 (1968).
[7] P.S. Landa, N.A. Miskunova, and Y.V. Ponomarev, Usp. Fiz. Nauk **132**, 601 (1980) [Sov. Phys. Usp. **23**, 813 (1980)].
[8] H. Achterberg and J. Michel, Ann. Phys. (Leipzig) **2**, 365 (1959).
[9] S. Pfau, A. Rutscher, and K. Wojaczek, Beitr. Plasmaphys. **9**, 333 (1969).
[10] K. Ohe and M. Hashimoto, J. Appl. Phys. **58**, 2975 (1985).
[11] C. Wilke, R.W. Leven, and H. Deutsch, Phys. Lett. A **136**, 114 (1989).
[12] T. Braun, J.A. Lisboa, and J.A.C. Gallas, Phys. Rev. Lett. **18**, 2770 (1992).
[13] B. Albrecht, H. Deutsch, R.W. Leven, and C. Wilke, Phys. Scr. **47**, 196 (1993).
[14] W.X. Ding, W. Huang, X.D. Wang, and C.X. Yu, Phys. Rev. Lett. **70**, 170 (1993).
[15] W.X. Ding, H. Deutsch, A. Dinklage, and C. Wilke, Phys. Rev. E **55**, 3769 (1997).
[16] K. Ohe, Curr. Top. Phys. Fluids **1**, 319 (1994).
[17] I. Grabec, Phys. Fluids **17**, 1834 (1974).
[18] I. Grabec and S. Mikac, Plasma Phys. **16**, 1155 (1974).
[19] K. Wojaczek, Beitr. Plasmaphys. **2**, 1 (1962); **2**, 13 (1962).
[20] L. Pekarek, K. Mašek, and K. Rohlena, Czech. J. Phys. B **20**, 879 (1970).
[21] T. Ružička and K. Rohlena, Czech. J. Phys. B **22**, 906 (1972).
[22] K. Rohlena, T. Ružička, and L. Pekarek, Czech. J. Phys. B **22**, 920 (1972).
[23] L.D. Tsendin, J. Tech. Phys. **52**, 635 (1982).
[24] L.D. Tsendin, J. Tech. Phys. **52**, 643 (1982).
[25] P.S. Landa, *Self-Oscillations in Distributed Systems* (Nauka, Novosibirsk, 1983).
[26] L. Pekarek, Czech. J. Phys. **8**, 742 (1958).
[27] H.D. Weltmann, T. Bräuer, H. Deutsch, and C. Wilke, Contrib. Plasma Phys. **35**, 225 (1995).
[28] J.P. Boeuf and L.C. Pitchford, Phys. Rev. E **51**, 1376 (1995).
[29] S. Pfau and A. Rutscher, Ann. Phys. (Leipzig) **22**, 166 (1969).
[30] T. Ružička, A. Rutscher, and S. Pfau, Ann. Phys. (Leipzig) **24**, 124 (1970).
[31] S. Pfau, J. Rohmann, D. Uhrlandt, and R. Winkler, Contrib. Plasma Phys. **36**, 449 (1996).
[32] B. Bruhn, B.P. Koch, and N. Goepp (unpublished).
[33] G. Iooss and M. Adelmeyer, *Topics in Bifurcation Theory* (World Scientific, Singapore, 1992).
[34] L.S. Tuckerman and D. Barkley, Physica D **46**, 57 (1990).
[35] S. Gubsch, Diploma thesis, Universität Greifswald, 1996 (unpublished).
[36] A. Dinklage, B. Bruhn, H. Deutsch, S. Gubsch, B.P. Koch, and C. Wilke (unpublished).
[37] D. Mönke, Diploma thesis, Universität Greifswald, 1993 (unpublished).
[38] S. Franke, Diploma thesis, Universität Greifswald, 1996 (unpublished).